Neuro-Oncology

19(9), 1195–1205, 2017 | doi:10.1093/neuonc/nox017 | Advance Access date 24 March 2017

Blocking MIR155HG/miR-155 axis inhibits mesenchymal transition in glioma

Xuechao Wu,[†] Yingyi Wang,[†] Tianfu Yu,[†] Er Nie, Qi Hu, Weining Wu, Tongle Zhi, Kuan Jiang, Xiefeng Wang, Xiaojie Lu, Hailin Li, Ning Liu, Junxia Zhang, and Yongping You

Department of Neurosurgery, The First Affiliated Hospital of Nanjing Medical University, Nanjing, China (Xc.W., Y.W., T.Y., E.N., Q.H., W.W., T.Z., K.J., Xf.W., H.L., N.L., J.Z., Y.Y.); Department of Neurosurgery, Wuxi Second Hospital Affiliated to Nanjing Medical University, Wuxi, China (Xc.W., X.L.)

Corresponding Authors: Yongping You, PhD, Department of Neurosurgery, The First Affiliated Hospital of Nanjing Medical University, Nanjing 210029, China (yypl9@njmu.edu.cn); and Junxia Zhang, PhD, Department of Neurosurgery, The First Affiliated Hospital of Nanjing Medical University, Nanjing 210029, China (zjx232@njmu.edu.cn).

[†]These authors contributed equally to this work.

Abstract

Background. MIR155 host gene (MIR155HG) is a long noncoding RNA that has been considered as the primary micro (mi)RNA of miR-155. MIR155HG plays an essential role in hematopoiesis, inflammation, and tumorigenesis. Our study investigated the clinical significance, biological function, mechanisms, and small-molecule inhibitors of the MIR155HG/miR-155 axis in glioma.

Methods. We analyzed the expression of the MIR155HG/miR-155 axis and the correlation with glioma grade and patient survival using 2 different glioma gene expression datasets. Biological significance was elucidated through a series of in vitro and in vivo experiments. Furthermore, we conducted a high-throughput screening for small molecules to identify a potential inhibitor of the MIR155HG/miR-155 axis.

Results. Increased MIR155HG was associated with glioma grade, mesenchymal transition, and poor prognosis. Functionally, MIR155HG reduction by small interfering RNA inhibited cell proliferation, migration, invasion, and orthotopic glioma growth by repressing the generation of its derivatives miR-155-5p and miR-155-3p. Bioinformatics and luciferase reporter assays revealed that protocadherin 9 and protocadherin 7, which act as tumor suppressors by inhibiting the Wnt/β-catenin pathway, were direct targets of miR-155-5p and miR-155-3p, respectively. Finally, we identified NSC141562 as a potent small-molecule inhibitor of the MIR155HG/miR-155 axis.

Conclusions. Our results demonstrate that the MIR155HG/miR-155 axis plays a critical role in facilitating glioma progression and serves as a prognostic factor for patient survival in glioblastoma. High-throughput screening indicated that the MIR155HG/miR-155 axis inhibitor NSC141562 may be a useful candidate anti-glioma drug.

Key words

glioma | mesenchymal transition | MIR155HG | small-molecule inhibitor | survival

Long noncoding RNAs (lncRNAs) are non-protein-coding transcripts consisting of more than 200 nucleotides in length and play key molecular roles in epigenetic regulations, including chromatin remodeling, transcriptional repression, and posttranscriptional regulation.[1] LncRNAs are pervasively implicated in different physiological and pathological processes, such as imprinting, immune response, cancer progression, and apoptosis control.[2–6]

MIR155 host gene (MIR155HG), an lncRNA, formerly known as BIC (B-cell integration cluster), was originally identified as a gene that was transcriptionally activated by promoter insertion at a common retroviral integration site in B-cell lymphomas induced by avian leukosis virus.[7] The

Importance of the study

Our study showed that increased MIR155HG was closely associated with glioma grade and mesenchymal transition and predicted a poor prognosis. Functionally, MIR155HG reduction by small interfering RNA inhibited cell proliferation, migration, invasion, and orthotopic glioma growth by repressing the generation of its derivatives miR-155-5p and miR-155-3p. Finally, we identified NSC141562, a potent small-molecule inhibitor of the MIR155HG/miR-155 axis, by high-throughput screening. To our knowledge, this is the first study to show the importance of the MIR155HG/miR-155 axis in glioma and represents a novel promising approach for blocking the MIR155HG/miR-155 axis for glioma therapy.

human homolog of this gene was cloned and characterized and consists of 3 exons within a 13-kb region located in chromosome 21q21, but it lacks an extensive open reading frame.[8] Examination of the RNA secondary structure of the conserved regions in exon 3 implied that these sequences formed hairpins containing imperfectly base-paired stem loops, suggesting that MIR155HG may function as a primary micro (mi)RNA for miR-155.[8] Recent studies have established that MIR155HG expression is activated by several transcriptional regulation factors, such as activator protein 1, myeloblastosis, nuclear factor-kappaB, and Smad4.[9–12] However, the biological function and mechanisms of MIR155HG in cancer are not fully known.

Epithelial-to-mesenchymal transition is a process that facilitates tumor metastasis and progression, and increasing studies have revealed its relationship with the development and progression of glioma.[13–17] We prefer to call it mesenchymal transition, due to glioma not being of epithelial origin. In the current study, we found that the MIR155HG/miR-155 axis was closely correlated with glioma grade, mesenchymal transition, and poor prognosis, and identified NSC141562, a potent small-molecule inhibitor of the MIR155HG/miR-155 axis. Thus, the oncogenic function of the MIR155HG/miR-155 axis may serve as a potential target for glioma therapy.

Materials and Methods

Human Tissue Samples and Cell Lines

In total, 225 glioma data with mRNA expression microarray were downloaded from the Chinese Glioma Genome Atlas (CGGA) data portal (http://www.cgga.org.cn, accessed February 21, 2017). Among all the samples, 158 gliomas contain miRNA expression data. Glioma gene expression datasets deposited at the Repository of Molecular Brain Neoplasia Data (REMBRANDT; http://caintegrator.nci.nih.gov/rembrandt/, accessed February 21, 2017) were also included in this study. Ten normal brain tissues (NBTs) and 10 primary glioblastoma (GBM) samples were obtained from the Department of Neurosurgery, The First Affiliated Hospital of Nanjing Medical University. Written informed consent was obtained from all patients. Our study was approved by the institutional review board and the ethics committee of Nanjing Medical University. The human U87 and U251 GBM cell lines were purchased from the Chinese Academy of Sciences Cell Bank. The primary GBM cells (pGBM-1) were established from a primary GBM surgical specimen.

Significance Analysis of Microarray and Gene Set Enrichment Analysis

The Significance Analysis of Microarray (SAM) was performed using a 2-class *t*-test in the R program (version 3.1.2) to identify differentially expressed genes in different MIR155HG expression groups. The Gene Set Enrichment Analysis (GSEA) of the differentially expressed genes was performed using software downloaded from the Broad Institute (http://www.broadinstitute.org/gsea/index.jsp, accessed February 21, 2017) with C2 (curated gene sets) and C5 (Gene Ontology gene sets) collections.

Oligonucleotides, Plasmids, and Transfection

The MIR155HG small interfering (si)RNA, and inhibitor, mimics and negative control (NC) RNAs of miR-155-5p and miR-155-3p were synthesized and purified by GenePharma. The RNA sequences mentioned above were as follows: si-MIR155HG: sense, 5′-CUGGGAUGUUCAACCUUAATT-3′, antisense, 5′-UUAAGGUUGAACAUCCCAGTT-3′; miR-155-5p inhibitor (anti–miR-155-5p): 5′-ACCCCUAUCACGAUUAGCAUUAA-3′, miR-155-5p mimics: sense, 5′-UUAAUGCUAAUCGUGAUAGGGGU-3′, antisense, 5′-CCCUAUCACGAUUAGCAUUAAUU-3′; miR-155-3p inhibitor (anti–miR-155-3p): 5′-UGUUAAUGCUAAUAUGUAGGAG-3′, miR-155-3p mimics: sense, 5′-CUCCUACAUAUUAGCAUUAACA-3′ , antisense, 5′-UUAAUGCUAAUAUGUAGGAGUU-3′. An siRNA that was unrelated to any human sequence was used as an NC: sense, 5′-UUCUCCGAACGUGUCACGUTT-3′,antisense:5′-ACGUGACACGUUCGGAGAATT-3′; miRNA inhibitor negative control (anti-NC): 5′-CAGUACUUUUGUGUAGUACAA-3′.

The protocadherin (PCDH)9 and PCDH7 overexpression plasmids (pcDNA3.1-PCHD9, pcDNA3.1-PCHD7), which included the full-length protein coding sequences, were constructed by GeneChem. Oligonucleotides and plasmids were transfected into cells using Lipofectamine 2000 (Invitrogen) following the manufacturer's instructions.

Cell Experiments

RNA extraction, quantitative real-time (RT)-PCR, Cell Counting Kit-8 assay, wound healing assay, transwell assay, western blot assay, luciferase reporter assay, and assay by MTT (3-(4,5-dimethylthiazol-2-yl)-2,5-diphenyltetrazolium bromide) are described in the Supplementary material.

Orthotopic Glioma Model and Treatment

Female nude mice at 4–6 weeks of age were used in this experiment, following the standard guidelines under a protocol approved by Nanjing Medical University. Lentivirus containing siMIR155HG segments (Lenti-siMIR155HG; siRNA sequence is 5′-CUGGGAUGUUCAACCUUAATT-3′) or NC sequence (Lenti-NC; negative control sequence is 5′-UUCUCCGAACGUGUCACGUTT-3′) was obtained from GeneChem. A total of 0.5×10^5 U87 cells were co-infected with lentiviruses expressing luciferase and a Lenti-NC or Lenti-siMIR155HG and then implanted stereotactically to establish intracranial gliomas. Mice were imaged for Fluc activity using bioluminescence imaging on days 3, 7, 14, 21, and 28.

High-Throughput Molecular Dockings

The hairpin loop of the pre–miR-155 was chosen to build the 3D structure using the MC-Fold/MC-Sym pipeline.[18] High-throughput molecular dockings for pre–miR-155 against the 1990 National Cancer Institute/diversity compounds were conducted using the AutoDock program. Protein–ligand interactions were analyzed and visualized using Jmol (http://jmol.sourceforge.net/, accessed February 21, 2017). Detailed high-throughput screening is described in the Supplementary materials.

Statistical Analysis

All data shown in the graphs are presented as mean ± standard error of 3 independent experiments. The 2-sided Student's *t*-test was used to determine differences between 2 groups and one-way ANOVA was used to test differences among at least 3 groups. The log-rank test was employed to assess the statistical significance between stratified survival groups using the median value as the cutoff in a Kaplan–Meier analysis. Cox proportional hazards regression analyses were performed using SPSS software, and Pearson correlation was used to determine significant differences. $P < .05$ was considered significant for all statistical analysis.

Results

Increased MIR155HG Expression Correlates with Glioma Grade

To examine MIR155HG expression in human glioma, we initially analyzed the whole genome gene profiling of 5 normal and 220 glioma tissues in the CGGA dataset. As shown in Fig. 1A, GBM tissues showed significantly increased MIR155HG transcript levels compared with normal tissues ($P = .0051$). Moreover, MIR155HG expression was significantly higher in high-grade glioma (HGG) than in low-grade glioma (LGG) (grade IV vs grade II, $P < .001$; grade III vs grade II, $P = .0216$). We next examined the association between MIR155HG expression level and glioma grade in another independent glioma gene expression dataset, REMBRANDT. We found that MIR155HG was significantly associated with tumor grade (one-way $P < .0001$), which was consistent with the CGGA data. Together these findings suggest that MIR155HG may play an important role in glioma progression.

MIR155HG Is an Independent Prognostic Factor for GBM Patients

To investigate the correlation between MIR155HG expression and overall survival, we conducted Kaplan–Meier survival curve analysis with a log-rank comparison in the CGGA and REMBRANDT datasets. A total of 83 primary GBMs with complete survival data in the CGGA set were divided into the high MIR155HG expression group ($n = 42$) and the low expression group ($n = 41$) based on the median ratio of relative MIR155HG expression in tumor tissues. We found that high expression of MIR155HG was inversely correlated with overall survival ($P = .0196$, Fig. 1B). Similar results were detected in the REMBRANDT data ($P = .0065$). These data indicated that overexpression of MIR155HG conferred a poor prognosis in GBM patients.

We next examined the relationship between MIR155HG expression and the features of clinical and molecular pathology of the 83 primary GBMs mentioned above. As shown in Supplementary Table S1, the expression of MIR155HG was significantly associated with male sex ($P = .011$) and wild-type isocitrate dehydrogenase 1 (IDH1) ($P = .001$), and was independent of the rest of the features. We then conducted a univariate Cox regression analysis using clinical and genetic variables for 83 primary GBMs and found that high expression of MIR155HG, high KPS score, and total resection were remarkably associated with overall survival, while gender or IDH1 mutation showed no association (Table 1).

Then we performed a multivariate Cox proportional hazards model to evaluate the factors that contributed to overall survival. MIR155HG expression, KPS score, and expression of proliferating cell nuclear antigen were correlated independently with overall survival (hazard ratio [HR] = 2.082, $P = .023$; HR = 0.450, $P = .016$; and HR = 2.455, $P = .014$, respectively) when considering age, resection, epidermal growth factor receptor, Ki-67, topoisomerase type II, and glutathione S-transferase pi ($P < .3$, univariate Cox regression analysis) (Table 1). Together these results implied that MIR155HG may serve as an independent prognostic factor for GBM patients.

MIR155HG Is a Mesenchymal Transition–Associated Long Noncoding RNA

Using the expression data from the CGGA dataset, we identified 1858 upregulated genes and 2120 downregulated genes in the high MIR155HG expression group (SAM, false discovery rate < 5%, fold change > 2; Fig. 1C). We named these genes "MIR155HG differentially expressed genes." We performed GSEA to verify whether we could detect differences in the mesenchymal transition–associated genes listed by Cheng[19] in the CGGA data, and we found that these genes were indeed significantly enriched in HGG compared with LGG ($P < .0001$, Supplementary Fig. S1A). Further, GSEA of the MIR155HG differentially expressed genes demonstrated remarkable enrichments in mesenchymal transition–associated genes in the high MIR155HG expression samples of GBM ($P < .0001$; Fig. 1D and Supplementary Fig. S1B).

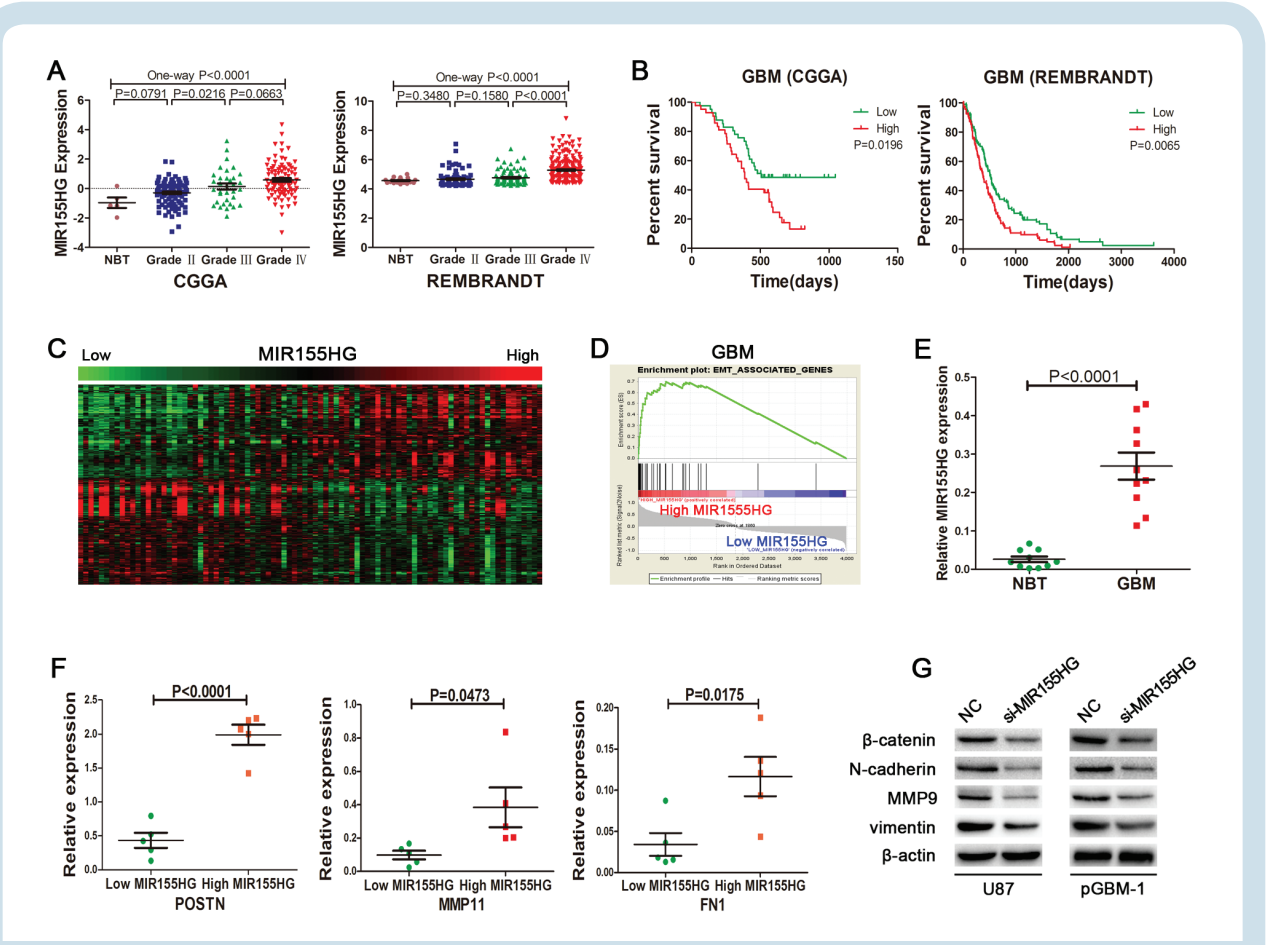

Fig. 1 Increased MIR155HG expression correlates with glioma grade and mesenchymal transition and confers a poor prognosis in GBM patients. (A) The level of MIR155HG was analyzed in glioma tissues of the CGGA and REMBRANDT glioma datasets. (B) Kaplan–Meier survival curves for MIR155HG expression in GBM tissues of the CGGA and REMBRANDT datasets. (C) In silico analysis of MIR155HG mRNA expression and the correlation with its associated genes in glioma of CGGA datasets. A heatmap of relative expression of MIR155HG differentially expressed genes in glioma tissues sorted by level of MIR155HG expression. (D) GSEA analysis showed that there was enriched expression of mesenchymal transition–associated genes in high MIR155HG expression samples of GBM. (E) The expression of MIR155HG in 10 primary GBM samples is higher than that in 10 normal brain tissues. (F) The expressions of POSTN, MMP11, and FN1 are increased in GBM samples with high MIR155HG expression compared with those with low MIR155HG expression. (G) Decreased expression of MIR155HG regulated the expression of common mesenchymal transition–associated markers in U87 and primary GBM cells.

GSEA was then performed to identify Gene Ontology terms and Kyoto Encyclopedia of Genes and Genomes and Reactome pathways that were differentially regulated by MIR155HG differentially expressed genes between the high MIR155HG expression group and the low expression group. The GSEA results revealed many mesenchymal transition–related categories (extracellular matrix, extracellular region, cell migration, response to wounding, extracellular matrix receptor interaction, and focal adhesion) (Supplementary Fig. S1C and D). Additionally, GSEA indicated that 6 distinct published mesenchymal transition–related gene signatures[20–25] were significantly enriched in high MIR155HG expression samples, strongly suggesting that MIR155HG induced a pervasive and sustained mesenchymal transition signaling program (Supplementary Fig. S1E).The work flow of these analyses is shown in Supplementary Fig. S1F.

Ten NBTs and 10 primary GBM samples from patients were used to detect the expression status of MIR155HG by RT-PCR. As shown in Fig. 1E, the level of MIR155HG was significantly upregulated in these GBM specimens compared with the level in NBTs ($P < .0001$). We chose 3 mesenchymal transition–associated markers (POSTN, MMP11, and FN1) from Cheng's list and found higher expression levels in GBMs with high MIR155HG expression ($n = 5$) than those with low MIR155HG expression ($n = 5$) (Fig. 1F). Next, to directly test the functional role of MIR155HG in the mesenchymal transition, MIR155HG was downregulated by specific siRNA in glioma cells (Supplementary Fig. S2A). MIR155HG reduction triggered remarkable decrease of β-catenin, N-cadherin, vimentin, and matrix metalloproteinase 9 (Fig. 1G).These results strongly demonstrated that MIR155HG is a mesenchymal transition–associated lncRNA.

MIR155HG Promotes Glioma Progression In vitro and In vivo

We examined the role of MIR155HG in cell proliferation by Cell Counting Kit-8 assays. Cell proliferation was

Table 1 Cox regression analyses of MIR155HG expression and clinicopathologic characteristics in relation to GBM clinical outcome

Variable	Univariable Regression		Multivariable Regression	
	HR	*P*	HR	*P*
Gender, female/male	1.254	.412		
Increasing age	1.013	.277	1.010	.457
KPS score	0.331	<.001	0.450	.016
Total resection	0.558	.033	0.550	.118
High MIR155HG	1.900	.022	2.082	.023
High EGFR	1.529	.146	0.988	.971
High Ki-67	1.854	.062	2.128	.112
High PCNA	1.569	.124	2.455	.014
High TOPO II	1.535	.136	0.976	.953
High GST-Π	1.384	.243	1.277	.413
IDH1 mutation	0.639	.306		
MGMT promoter methylation	1.150	.695		
High MGMT	0.921	.782		

Abbreviations: EGFR, epidermal growth factor receptor; PCNA, proliferating cell nuclear antigen; TOPO II, topoisomerase II; GST-Π, glutathione S-transferase pi; MGMT, O^6-DNA methylguanine-methyltransferase.

dramatically suppressed in U87, U251, and primary GBM cells after transfection with siMIR155HG compared with NC cells (Supplementary Fig. S2B). Glioma cells transfected with siMIR155HG presented significantly reduced scratch wound healing and lower invasion abilities compared with NC (Fig. 2A and B and Supplementary Fig. S2C and D).

To further examine whether tumor growth was inhibited by siMIR155HG, we performed in vivo analyses using a U87 orthotopic glioma model. A statistically significant difference in tumor volume as indicated by bioluminescence imaging was detected between the Lenti-NC and Lenti-siMIR155HG treated groups (Fig. 2C). Representative images of mice implanted with intracranial tumors are shown in Fig. 2D. In addition, treating with Lenti-siMIR155HG was associated with significantly longer survival times in the mice (Fig. 2E).

MiR-155-5p and miR-155-3p Are Key Derivatives of MIR155HG

MIR155HG is the primary miRNA of miR-155, and thus we next examined miR-155 expression. MIR155HG knockdown remarkably reduced miR-155-5p and miR-155-3p expression in U87 and primary GBM cells (Fig. 3A). As shown in Supplementary Fig. S3A and B, Pearson correlation assay revealed a significant and positive correlation between MIR155HG and miR-155-5p or miR-155-3p in 158 gliomas and 64 GBM tissues. One-way ANOVA analysis showed that both miR-155-5p and miR-155-3p were significantly associated with tumor grade ($P = .0302$ and $P < .0001$, respectively) and their expression levels were higher in GBM than in LGG (Supplementary Fig. S3C). Moreover, high expression of miR-155-3p correlated with a worse survival outcome in GBM patients ($P = .0448$), while miR-155-5p expression did not show significant correlation with overall survival ($P = .8340$; Supplementary Fig. S3D). After the expression of miR-155-5p or miR-155-3p was downregulated by anti–miR-155-5p or anti–miR-155-3p transfection, respectively (Supplementary Fig. S4A), cell proliferation, migration, and invasion were remarkably suppressed in glioma cells (Fig. 3B and C and Supplementary Fig. S4B and C).

To determine whether the phenotypes associated with MIR155HG are mediated by miR-155-5p and miR-155-3p, we cotransfected siMIR155HG with miR-155-5p or miR-155-3p mimics. As shown in Fig. 3D and E and Supplementary Fig. S4D and E, overexpression of miR-155-5p or miR-155-3p markedly reversed the inhibition of cell proliferation, migration, and invasion induced by siMIR155HG. Collectively, these data suggested that miR-155-5p and miR-155-3p are critical participants in the biological function of MIR155HG in glioma.

MiR-155-5p or miR-155-3p Targets Protocadherin 9 or 7, Respectively

To explore downstream targets of miR-155-5p and miR-155-3p, we performed bioinformatics analysis using 2 online algorithms, TargetScan and microRNA, to predict mRNA targets. We found that PCDH9 contains putative binding sites in its 3′ untranslated region (UTR) for miR-155-5p, and PCDH7 contains putative binding sites for miR-155-3p (Fig. 4A). CGGA data revealed remarkable and negative correlation between miR-155-5p and PCDH9 and between miR-155-3p and PCDH7 (Supplementary Fig. S5A and B). Furthermore, reduced miR-155-5p or miR-155-3p expression in glioma cells led to an increase in PCDH9 or PCDH7 protein (Fig. 4B). Luciferase reporter assays showed that overexpression of miR-155-5p led to a marked decrease of luciferase activity of the PCDH9–3′

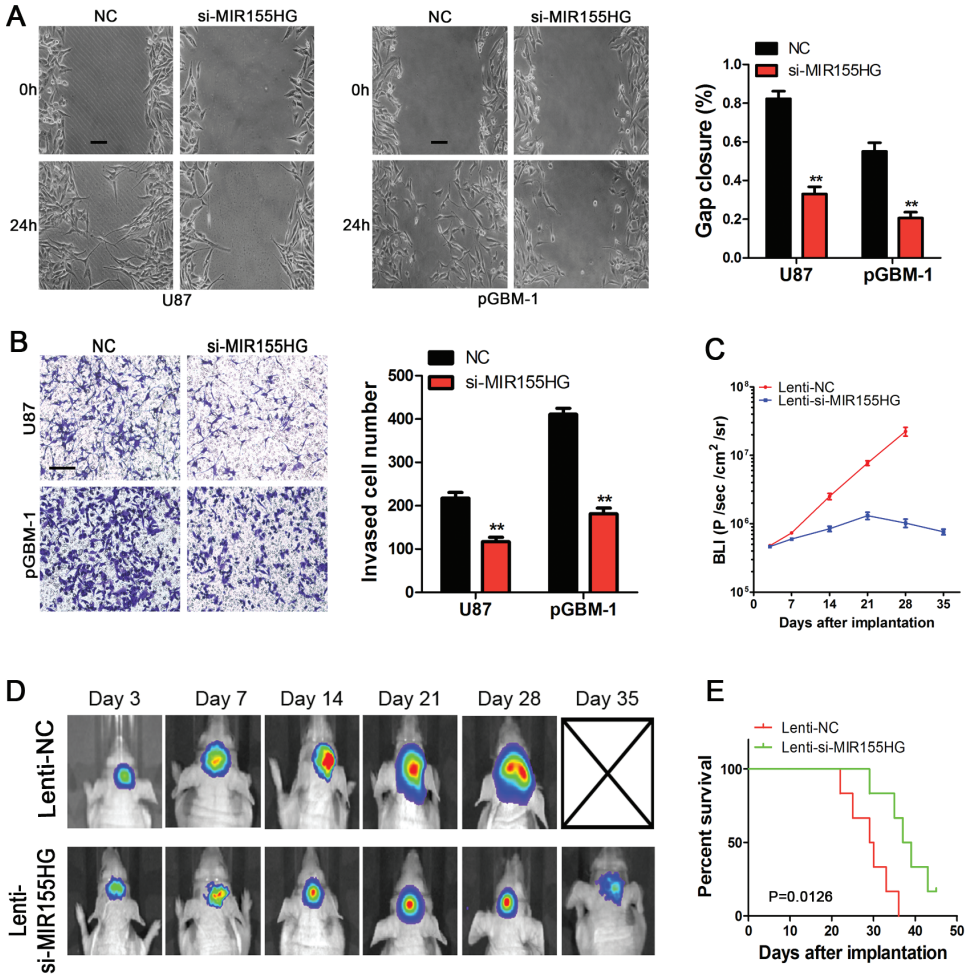

Fig. 2 MIR155HG knockdown inhibits glioma malignant phenotypes. (A) Wound healing assay of glioma cells transfected with control or siMIR155HG. The wound was photographed at different time points and wounded gaps were analyzed by measuring the distance of migrating cells for 3 different areas for each wound (scale bar: 100 μm). (B) SiMIR155HG inhibited the invasion of U87 and primary GBM cells. Cells were examined for cell invasion in 24-well plates with transwell chambers (scale bar: 200 μm). The invasiveness of glioma cells was attenuated after the decreased expression of MIR155HG. (C) Plot of the Fluc activity by bioluminescence imaging for intracranial tumors. (D) Representative images of mice implanted with intracranial tumors on days 3, 7, 14, 21, 28, and 35. (E) Overall survival of nude mice was determined by Kaplan–Meier survival curves, and the log-rank test was used to assess the statistical significance of the differences. $^{**}P < .01$.

UTR wild-type construct in U87 cells with no change in luciferase activity of PCDH9–3′ UTR mutant, which contains mutations in the putative binding sites (Fig. 4C). Similar data were observed with miR-155-3p. Our results strongly indicate that PCDH9 and PCDH7 are direct targets of miR-155-5p and miR-155-3p, respectively.

Protocadherin 9 and 7 Function as Tumor Suppressor Genes by Inhibiting the Wnt/β-catenin Signaling Pathway

PCDH9 and PCDH7 were significantly and reversely correlated with glioma grade and were remarkably downregulated in HGG in the CGGA and REMBRANDT datasets (Supplementary Fig. S6A and B). Low expression of PCDH7 showed a poor prognosis for GBM patients in accordance with miR-155-3p, while PCDH9 didn't show any association with prognosis for GBM patients, just like miR-155-5p (Supplementary Fig. S6C and D).

To test whether PCDH9 and PCDH7 mediate the biological function of miR-155 in glioma cells, PCDH9 and PCDH7 expression vectors were used in rescue experiments. The overexpression of PCDH9 and PCDH7 were validated by western blot (Supplementary Fig. S7). As shown in Supplementary Fig. S8A–F, overexpression of PCDH9 and PCDH7 suppressed glioma cell proliferation, migration, and invasion. These results were consistent with the effects of miR-155 reduction. Furthermore, when cells were cotransfected with miR-155-5p and PCDH9, or miR-155-3p and PCDH7, the effect of miR-155 in promoting cell proliferation, migration, and invasion was significantly attenuated. These results further suggested that

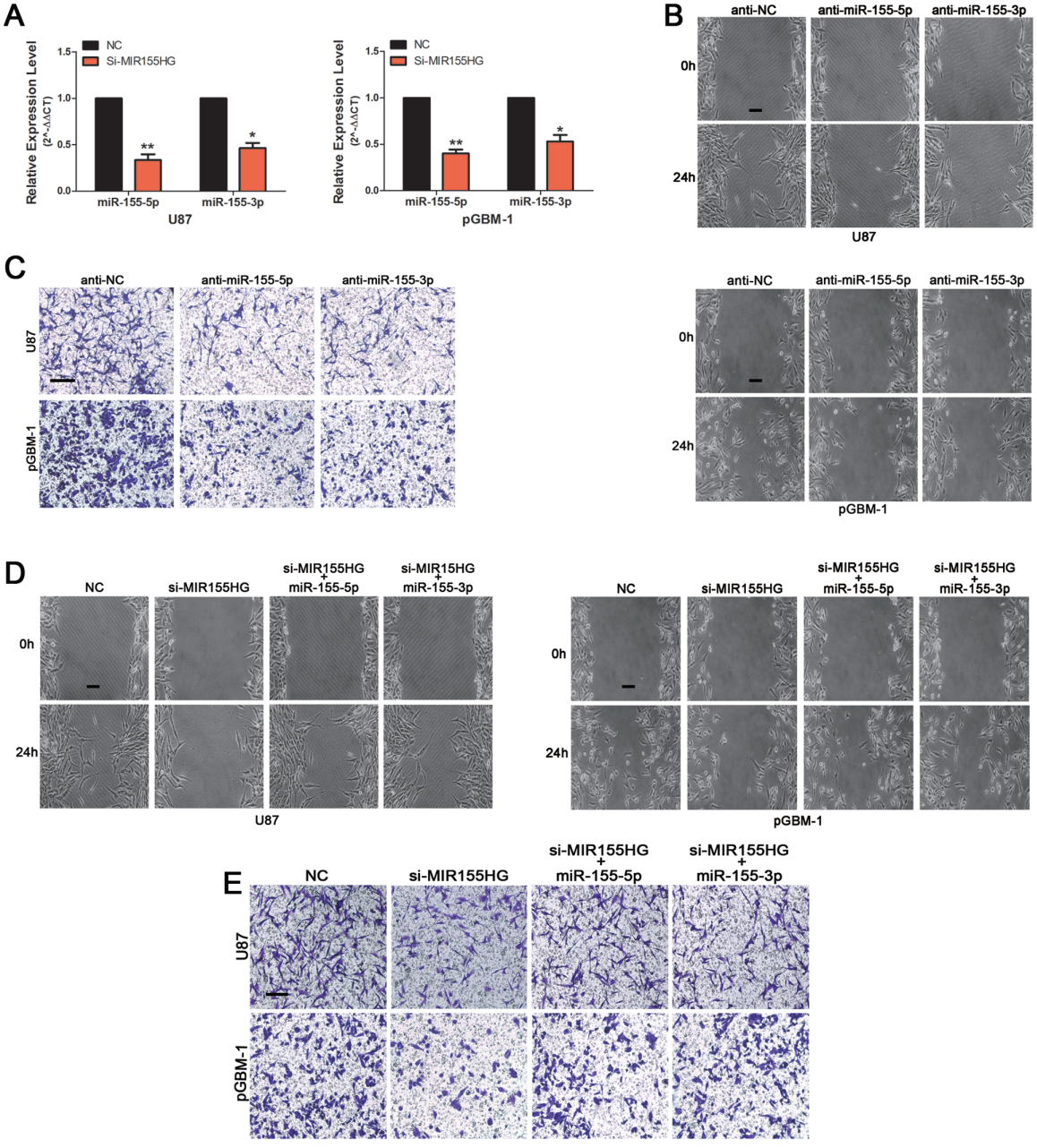

Fig. 3 MiR-155-5p and miR-155-3p are functionally relevant effectors of MIR155HG-induced cell proliferation and invasion. (A) MIR155HG knockdown remarkably reduced miR-155-5p and miR-155-3p expression in U87 and primary GBM cells. (B) Effect of anti–miR-155-5p and anti–miR-155-3p on cell migration (scale bar: 100 μm). (C) Cell invasion ability was analyzed after differential treatment via transwell assay (scale bar: 200 μm). (D and E) Overexpression of miR-155-5p and miR-155-3p reversed the siMIR155HG-induced inhibition of cell migration (scale bar: 100 μm) and invasion (scale bar: 200 μm).*$P < .05$, **$P < .01$, ***$P < .001$.

PCDH9 and PCDH7 are the functional downstream targets of miR-155.

To study the underlying mechanism, we performed western blot analyses of potential mediating factors. The results revealed that overexpression of PCDH9 and PCDH7 remarkably downregulated the expression of β-catenin and cyclin D1 and increased the levels of phosphorylated β-catenin (pβ-catenin) (Fig. 4D). Moreover, concomitant overexpression of miR-155-5p/-3p and PCDH9/7 abrogated the downregulation of pβ-catenin and upregulation of β-catenin and cyclin D1 reduced by miR-155-5p/-3p. Together, these data support the idea that PCDH9 and PCDH7, which are direct targets of miR-155, function as tumor suppressor genes by inhibiting the Wnt/β-catenin signaling pathway.

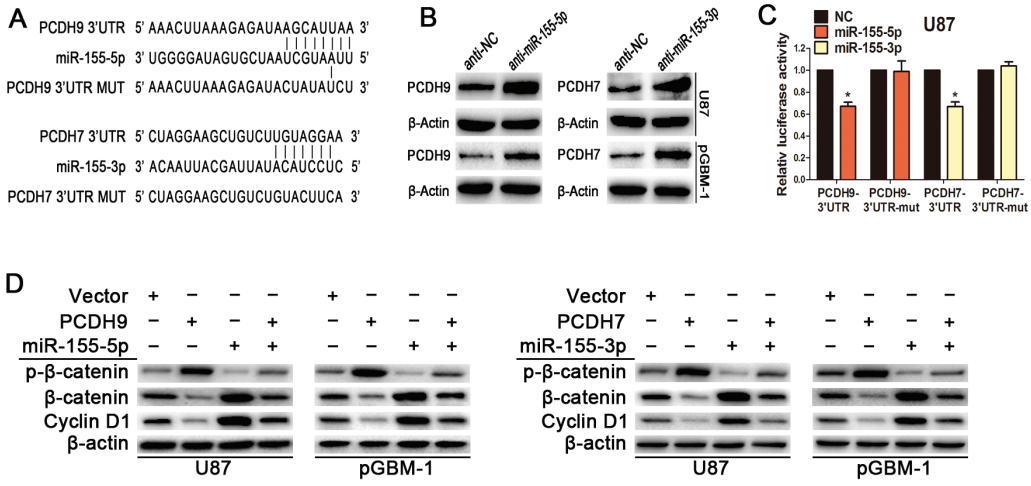

Fig. 4 PCDH9 and PCDH7 are the downstream target genes of miR-155 and function as tumor suppressors by inhibiting the Wnt/β-catenin signaling pathway. (A) Putative binding sites of miR-155-5p within the PCDH9 3′ UTR predicted by TargetScan, and putative binding sites of miR-155-3p within the PCDH7 3′ UTR predicted by microRNA. (B) Western blot analysis showed that PCDH9 and PCDH7 expression were upregulated after miR-155 expression was inhibited. (C) MiR-155-5p downregulated luciferase activities controlled by wild-type PCDH9 3′ UTR but did not affect luciferase activity controlled by mutant PCDH9 3′ UTR. And miR-155-3p downregulated luciferase activities controlled by wild-type PCDH7 3′ UTR but did not affect luciferase activity controlled by mutant PCDH7 3′ UTR. (D) Overexpression of PCDH9 and PCDH7 downregulated the expression of β-catenin and cyclin D1 and upregulated pβ-catenin expression. $^{*}P < .05$, $^{**}P < .01$, $^{***}P < .001$.

Identification of NSC141562 as a Potent Inhibitor of miR-155

To screen small-molecule inhibitors of the MIR155HG/miR-155 axis, we conducted a high-throughput screening based on the 3D structure of the Dicer binding site on pre–miR-155 for small molecules targeting miR-155. The sequence of the pre–miR-155 hairpin loop (Dicer binding site on pre–miR-155) was generated from the miRBase database and then input into the MC-Fold/MC-Sym pipeline to construct a 3D model (Supplementary Figure S9A). We conducted high-throughput molecular dockings for pre–miR-155 against the 1990 National Cancer Institute/diversity compounds using the AutoDock program (Supplementary Table S2). The specific docking process is shown in Supplementary Video S1. Here, our dockings revealed 8 compounds with high-binding affinity (Supplementary Table S3). In addition, NSC141562 showed the highest affinity with pre–miR-155. Supplementary Figure S9B and C display the chemical structure of NSC141562 and its highest affinity with the best docking pose.

We next conducted MTT assays to evaluate the impact of these 8 compounds on cell viability in U87 cells. All the screened compounds inhibited glioma cell viability in a dose-dependent manner after 48 h of treatment (Supplementary Table S4). The top 3 with the lowest half-maximal inhibitory concentration values (NSC141562, NSC35450, and NSC10408) were further assessed for miR-155 inhibition efficacy in U87 and primary GBM cells. NSC141562 presented the strongest inhibition of mature miR-155 generation in a time-dependent manner, with an approximate 50% inhibition after 6 h of treatment (Fig. 5A). Additionally, NSC141562-treated glioma cells showed reduced proliferation, migration, and invasion (Fig. 5B and C and Supplementary Fig. S9D and E). Overexpression of miR-155-5p largely reversed NSC141562-induced suppressive effects on glioma cells (Supplementary Fig. S10A–D). Furthermore, we found that NSC141562 treatment increased the expression of PCDH9 and PCDH7, whereas it decreased the expression of mesenchymal transition–associated markers, N-cadherin, vimentin, matrix metalloproteinase 9, and β-catenin (Fig. 5D). These data suggested NSC141562 as a potent small-molecule inhibitor of the MIR155HG/miR-155 axis.

Discussion

MIR155HG has been characterized as a vital regulatory factor involved in several physiological and pathological processes, such as hematopoiesis, inflammation, immunity, and tumor occurrence and development.[10,26–29] In our study, MIR155HG was positively associated with tumor grade and represented an independent adverse prognostic factor in GBM patients. MIR155HG repression inhibited glioma growth in vitro and in vivo. GSEA and in vitro experiments demonstrated that MIR155HG regulated mesenchymal transition progression.

Tam[8] demonstrated that MIR155HG lacked conserved open reading frames but did have a conserved secondary RNA structure located within exon 3. These sequences formed hairpins containing imperfect base-paired stem loops, suggesting that MIR155HG might function as the primary miRNA precursor of miR-155. Eis et al[30] confirmed that miR-155 was indeed processed from the MIR155HG transcript in humans by ectopic MIR155HG expression in

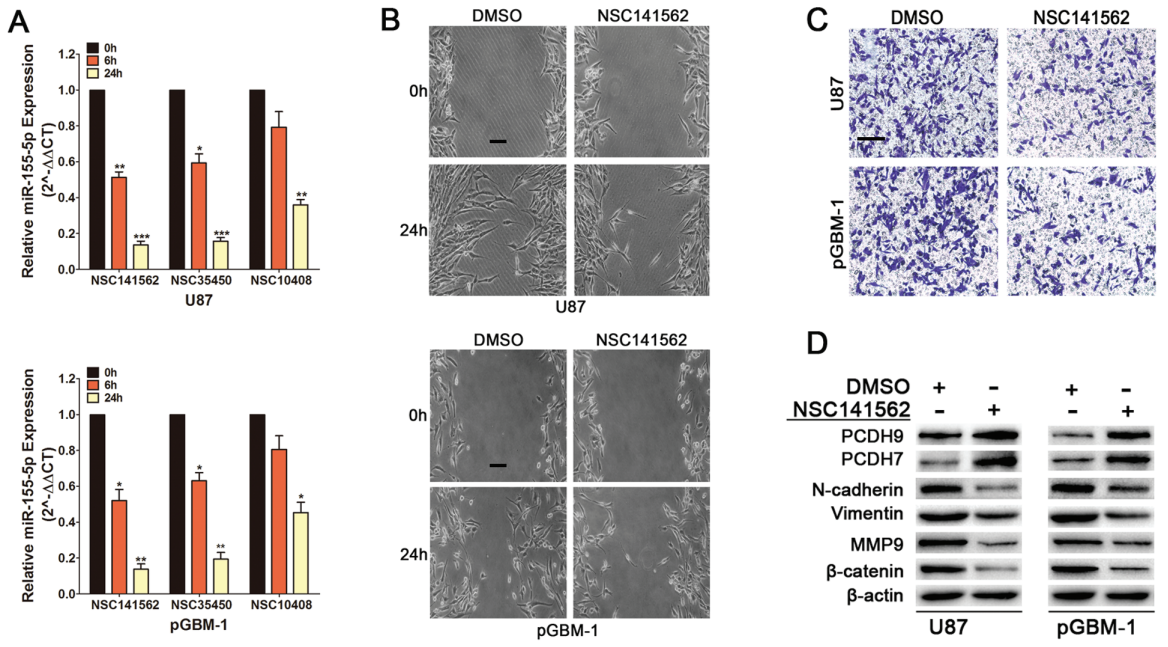

Fig. 5 NSC141562 is a potent inhibitor of the MIR155HG/miR-155 axis. (A) MiR-155-5p relative expression assayed using RT-PCR after small-molecule inhibitor treatment at a half-maximal inhibitory concentration dose in U87 and primary GBM cells. (B and C) The results of wound healing assay (scale bar: 100 μm) and transwell assay (scale bar: 200 μm) showed that NSC141562 suppressed glioma cell migration and invasion. (D) Western blot assays revealed that NSC141562 significantly increased PCDH9/7 expression and decreased the expression of mesenchymal transition–associated markers. $^{*}P < .05$, $^{**}P < .01$, $^{***}P < .001$.

a MIR155HG and miR-155 negative cell line. In this study, we showed that both miR-155-5p and miR-155-3p were elevated in HGG tissues compared with LGG tissues and were positively correlated with MIR155HG expression in the CGGA data. In vitro experiments showed that deprivation of MIR155HG expression remarkably reduced miR-155-5p and miR-155-3p expression in glioma cells. Such correlation is in agreement with the previous findings showing that MIR155HG is the precursor of miR-155. Moreover, our results demonstrated that miR-155-5p and miR-155-3p largely abrogated the siMIR155HG-induced inhibition of cell proliferation, migration, and invasion. Previous studies have demonstrated the promotion effect of miR-155 on glioma development and progression and identified many novel targets—for example, FOXO3a, MXI1, and HBP1.[31–33] In our study, we found that miR-155-5p and -3p directly target PCDH9 and 7, which play a pivotal role in glioma by suppressing the Wnt/β-catenin pathway. Given that miR-155-5p has been considered the only functional miR-155 form and the importance of miR-155-3p has been largely ignored, our study for the first time revealed that miR-155-3p could have similar function as miR-155-5p in glioma. In short, the present study confirmed the important correlation between MIR155HG and miR-155, and the crucial role of miR-155 in the biological function of MIR155HG.

To date, specific lncRNA inhibition has been mainly observed with siRNA,[34] while antisense miRNAs and locked nucleic acid anti-miRNAs and antagomirs are employed in the majority of miRNA inhibition.[35,36] Successful results in vitro and in vivo have been reported with these agents. However, the high cost of these methods is still a challenge for their use in preclinical research. Thus, it is urgent to explore small-molecule inhibitors targeting noncoding RNA as potential and novel drugs. Gumireddy and colleagues[37] screened more than 1000 compounds, conducted structure-activity relationship analyses, and identified diazobenzene and its derivatives as effective inhibitors of miR-21. Parisien and Major[18] proposed a new RNA-structure-prediction method based on the nucleotide cyclic motif implemented as a pipeline of 2 computer programs: MC-Fold and MC-Sym. Recently, we predicted the structure of pre–miR-21 and conducted an in silico high-throughput screen for small molecules that block miR-21 maturation. We identified a specific small-molecule inhibitor of miR-21, which was termed AC1MMYR2.[38] Here we applied this high-throughput screening method and identified a potent inhibitor of the MIR155HG/miR-155 axis, NSC141562, which showed remarkable inhibition efficacy of mature miR-155 generation, glioma cell proliferation, migration, and invasion by suppressing the Wnt/β-catenin signaling pathway (Supplementary Fig. S10E).

To our knowledge, ours is the first study to show that MIR155HG is a favorable factor for malignant progression, mesenchymal transition, and poor prognosis in glioma patients and exhibits pro-oncogenic activity by deriving miR-155-5p/-3p. We also identified NSC141562 as a potent small-molecule inhibitor of the MIR155HG/miR-155 axis by high-throughput screening. These findings represent a novel and promising approach for combinatorial therapy of glioma through the silencing of the MIR155HG/miR-155 axis.

Supplementary Material

Supplementary material is available at *Neuro-Oncology* online.

Funding

This work was supported by grants from the Research Special Fund for Public Welfare Industry of Health (201402008), the National Key Research and Development Plan (2016YFC0902500), National Natural Science Foundation of China (81672501, 81472362, 81302184, 81302185), Jiangsu Province's Natural Science Foundation (20131019, 20151585), the Program for Advanced Talents within Six Industries of Jiangsu Province (2015-WSN-036, 2016-WSW-013), and the Priority Academic Program Development of Jiangsu Higher Education Institutions.

Conflict of interest statement. The authors declare that they have no competing financial interests.

References

1. Yoon JH, Abdelmohsen K, Gorospe M. Posttranscriptional gene regulation by long noncoding RNA. *J Mol Biol*. 2013;425(19):3723–3730.
2. Prensner JR, Chinnaiyan AM. The emergence of lncRNAs in cancer biology. *Cancer Discov*. 2011;1(5):391–407.
3. Rossi MN, Antonangeli F. LncRNAs: new players in apoptosis control. *Int J Cell Biol*. 2014;2014:473857.
4. Beckedorff FC, Amaral MS, Deocesano-Pereira C, Verjovski-Almeida S. Long non-coding RNAs and their implications in cancer epigenetics. *Biosci Rep*. 2013;33(4):pii: e00061.
5. Sleutels F, Zwart R, Barlow DP. The non-coding Air RNA is required for silencing autosomal imprinted genes. *Nature*. 2002;415(6873):810–813.
6. Heward JA, Lindsay MA. Long non-coding RNAs in the regulation of the immune response. *Trends Immunol*. 2014;35(9):408–419.
7. Tam W, Ben-Yehuda D, Hayward WS. Bic, a novel gene activated by proviral insertions in avian leukosis virus-induced lymphomas, is likely to function through its noncoding RNA. *Mol Cell Biol*. 1997;17(3):1490–1502.
8. Tam W. Identification and characterization of human BIC, a gene on chromosome 21 that encodes a noncoding RNA. *Gene*. 2001;274(1–2):157–167.
9. Yin Q, Wang X, McBride J, Fewell C, Flemington E. B-cell receptor activation induces BIC/miR-155 expression through a conserved AP-1 element. *J Biol Chem*. 2008;283(5):2654–2662.
10. Vargova K, Curik N, Burda P, et al. MYB transcriptionally regulates the miR-155 host gene in chronic lymphocytic leukemia. *Blood*. 2011;117(14):3816–3825.
11. Thompson RC, Vardinogiannis I, Gilmore TD. Identification of an NF-κB p50/p65-responsive site in the human MIR155HG promoter. *BMC Mol Biol*. 2013;14:24.
12. Kong W, Yang H, He L, et al. MicroRNA-155 is regulated by the transforming growth factor beta/Smad pathway and contributes to epithelial cell plasticity by targeting RhoA. *Mol Cell Biol*. 2008;28(22):6773–6784.
13. Meng J, Li P, Zhang Q, Yang Z, Fu S. A radiosensitivity gene signature in predicting glioma prognostic via EMT pathway. *Oncotarget*. 2014;5(13):4683–4693.
14. Liu Y, Hu H, Wang K, et al. Multidimensional analysis of gene expression reveals TGFB1I1-induced EMT contributes to malignant progression of astrocytomas. *Oncotarget*. 2014;5(24):12593–12606.
15. Praveen Kumar VR, Sehgal P, Thota B, Patil S, Santosh V, Kondaiah P. Insulin like growth factor binding protein 4 promotes GBM progression and regulates key factors involved in EMT and invasion. *J Neurooncol*. 2014;116(3):455–464.
16. Siebzehnrubl FA, Silver DJ, Tugertimur B, et al. The ZEB1 pathway links glioblastoma initiation, invasion and chemoresistance. *EMBO Mol Med*. 2013;5(8):1196–1212.
17. Song Y, Luo Q, Long H, et al. Alpha-enolase as a potential cancer prognostic marker promotes cell growth, migration, and invasion in glioma. *Mol Cancer*. 2014;13:65.
18. Parisien M, Major F. The MC-Fold and MC-Sym pipeline infers RNA structure from sequence data. *Nature*. 2008;452(7183):51–55.
19. Cheng WY, Kandel JJ, Yamashiro DJ, Canoll P, Anastassiou D. A multicancer mesenchymal transition gene expression signature is associated with prolonged time to recurrence in glioblastoma. *PLoS One*. 2012;7(4):e34705.
20. Jechlinger M, Grunert S, Tamir IH, et al. Expression profiling of epithelial plasticity in tumor progression. *Oncogene*. 2003;22(46):7155–7169.
21. Gotzmann J, Fischer AN, Zojer M, et al. A crucial function of PDGF in TGF-beta-mediated cancer progression of hepatocytes. *Oncogene*. 2006;25(22):3170–3185.
22. Sarrió D, Rodriguez-Pinilla SM, Hardisson D, Cano A, Moreno-Bueno G, Palacios J. Epithelial-mesenchymal transition in breast cancer relates to the basal-like phenotype. *Cancer Res*. 2008;68(4):989–997.
23. Alonso SR, Tracey L, Ortiz P, et al. A high-throughput study in melanoma identifies epithelial-mesenchymal transition as a major determinant of metastasis. *Cancer Res*. 2007;67(7):3450–3460.
24. Wu Y, Siadaty MS, Berens ME, Hampton GM, Theodorescu D. Overlapping gene expression profiles of cell migration and tumor invasion in human bladder cancer identify metallothionein 1E and nicotinamide N-methyltransferase as novel regulators of cell migration. *Oncogene*. 2008;27(52):6679–6689.
25. Anastassiou D, Rumjantseva V, Cheng W, et al. Human cancer cells express Slug-based epithelial-mesenchymal transition gene expression signature obtained in vivo. *BMC Cancer*. 2011;11:529.
26. Hu YL, Fong S, Largman C, Shen WF. HOXA9 regulates miR-155 in hematopoietic cells. *Nucleic Acids Res*. 2010;38(16):5472–5478.
27. Kohlhaas S, Garden OA, Scudamore C, Turner M, Okkenhaug K, Vigorito E. Cutting edge: the Foxp3 target miR-155 contributes to the development of regulatory T cells. *J Immunol*. 2009;182(5):2578–2582.
28. van den Berg A, Kroesen BJ, Kooistra K, et al. High expression of B-cell receptor inducible gene BIC in all subtypes of Hodgkin lymphoma. *Genes Chromosomes Cancer*. 2003;37(1):20–28.
29. Chang S, Wang RH, Akagi K, et al.; Kathleen Cuningham Foundation Consortium for Research into Familial Breast Cancer (kConFab). Tumor suppressor BRCA1 epigenetically controls oncogenic microRNA-155. *Nat Med*. 2011;17(10):1275–1282.
30. Eis PS, Tam W, Sun L, et al. Accumulation of miR-155 and BIC RNA in human B cell lymphomas. *Proc Natl Acad Sci U S A*. 2005;102(10):3627–3632.
31. Ling N, Gu J, Lei Z, et al. MicroRNA-155 regulates cell proliferation and invasion by targeting FOXO3a in glioma. *Oncol Rep*. 2013;30(5):2111–2118.
32. Zhou J, Wang W, Gao Z, et al. MicroRNA-155 promotes glioma cell proliferation via the regulation of MXI1. *PLoS One*. 2013;8(12):e83055.

33. Yan Z, Che S, Wang J, Jiao Y, Wang C, Meng Q. MiR-155 contributes to the progression of glioma by enhancing Wnt/β-catenin pathway. *Tumour Biol*. 2015;36(7):5323–5331.
34. Zhang JX, Han L, Bao ZS, et al.; Chinese Glioma Cooperative Group. HOTAIR, a cell cycle–associated long noncoding RNA and a strong predictor of survival, is preferentially expressed in classical and mesenchymal glioma. *Neuro Oncol*. 2013;15(12):1595–1603.
35. Yang M, Mattes J. Discovery, biology and therapeutic potential of RNA interference, microRNA and antagomirs. *Pharmacol Ther*. 2008;117(1):94–104.
36. Obad S, dos Santos CO, Petri A, et al. Silencing of microRNA families by seed-targeting tiny LNAs. *Nat Genet*. 2011;43(4):371–378.
37. Gumireddy K, Young DD, Xiong X, Hogenesch JB, Huang Q, Deiters A. Small-molecule inhibitors of microrna miR-21 function. *Angew Chem Int Ed Engl*. 2008;47(39):7482–7484.
38. Shi Z, Zhang J, Qian X, et al. AC1MMYR2, an inhibitor of Dicer-mediated biogenesis of oncomir miR-21, reverses epithelial-mesenchymal transition and suppresses tumor growth and progression. *Cancer Res*. 2013;73(17):5519–5531.